International Journal of Sciences

Research Article Volume 13 – September 2024 (09)

Joint Estimation of SOC and SOH for Li-ion Batteries Based on the Dual Kalman Filter Method

Haolong Pang[1]

[1]University of Manchester, United Kingdom

Abstract: With the widespread use of batteries, many of the devices in our lives rely on them. However, due to the variety and cost of batteries and their impact on the environment, we cannot use them in all devices. In order to ensure that the battery pack can work safely and reliably, the state of charge (SOC) and the state of health (SOH) of the battery must be accurately estimated. In this paper, we use lithium iron phosphate batteries as the research object. By analysing and comparing common battery models in the market, we obtain a second-order Thevenin equivalent circuit model suitable for this research and apply the forgetting factor recursive least squares method (FFRLS) to the parameters. In this paper, the SOC and SOH of the Li-ion battery are jointly simulated and validated using the double extended Kalman filter algorithm, the double particle filter algorithm and the double volume Kalman filter algorithm, and the results of the three algorithms are compared and analysed. The final results of the experiments show that, compared with the other two algorithms, the joint estimation of SOC and SOH of Li-ion batteries using the two-particle filter algorithm can accurately follow the true value, and the maximum absolute error and the average absolute error can be kept within 1%, and the estimation accuracy is more accurate compared with the other algorithms, and the performance of the algorithm effect is superior, meeting the accuracy and The performance of the algorithm is superior and meets the requirements of accuracy and stability of lithium-ion battery state estimation, which plays a reference role for future scientific research related to the development of new energy industry.

Keywords: Lithium-ion Battery, State of Charge, Battery Model, State of Health, Dual Kalman Filter

1 Introduction

1.1 Research background and significance

At present, people are facing a series of problems such as increasingly serious energy crisis and global warming. In order to achieve energy saving and reduce energy consumption, reduce pollution to nature, and develop energy saving and environmental protection, the development of new energy vehicles relying on power batteries has become the main direction of the automobile industry. With the development of modern information technology, mobile phones, laptops, medical equipment, A large number of new computer-controlled electronic equipment and equipment, such as earth satellites and high-frequency synchronous satellites, have been put into use, further promoting the rapid development and innovation of lithium-ion battery technology. At present, the application field of lithium-ion battery has gradually expanded to electric vehicles, aerospace and energy storage**Error! Reference source not found.**. According to the China Association of Automobile Manufacturers, the production and sales volume of China's new energy vehicles in 2018 were 3.219 million and 3.051 million respectively, up 20.8 percent and 18.5 percent year-on-year, and it is estimated that the scale of China's lithium battery industry will exceed 600 billion yuan by 2025. Lithium power batteries have high energy, low pollution and high safety, and have become one of the main power sources of new energy vehicles[1]. At present, people pay more and more attention to the safety of electric vehicles, so in order to increase the reliability of electric vehicles under complex working conditions, extend the life of power batteries, and increase the endurance of power batteries, reasonably and accurately estimate the State of Charge of batteries. SOC and State of Health (SOH) have also become hot topics in today's society.

The joint estimation of SOC and SOH of lithium batteries is relatively rare in the research so far, so it makes up for the deficiency in this aspect and achieves innovation. In order to ensure the improvement of the reliability of lithium batteries at work, the accurate estimation of the health status of lithium batteries and the real-time prediction of the remaining life are of great significance for the safe operation of lithium battery system and the reduction of operation and maintenance costs, which may lead to over-charging or over-discharging of the battery, which will lead to irreversible damage to the internal battery, reduce its service life, and even lead to explosion. The scientific and effective evaluation and management of the health status of lithium batteries will greatly improve the safety of lithium batteries. Reduce the extravagance of resources[2].

In order to improve the accuracy of the model, combined with the time-varying characteristics of the state and parameters of the model, this paper introduces the double Kalman filter algorithm and particle filter algorithm, and applies the double extended Kalman filter (DEKF), double particle filter (DPF) and double volume Kalman filter (DCKF) to jointly estimate SOC and SOH respectively. The convergence and accuracy of the two methods are compared, which plays a reference role in the future scientific research on the development

Published at: http://www.ijsciences.com/pub/issue/2024-09/
DOI: 10.18483/ijSci.2797; Online ISSN: 2305-3925; Print ISSN: 2410-4477

Haolong Pang (Correspondence)
+

of new energy industry.

1.2 Current status of SOC and SOH estimation

The state of charge of lithium-ion batteries cannot be directly measured by any instrument, so it is very difficult to estimate SOC. Similarly, the health status of lithium-ion batteries will be affected by various factors inside the battery, such as the temperature of the battery, the internal resistance of the battery and so on. Therefore, it is also difficult to estimate SOH, which has also aroused in-depth discussion among researchers at home and abroad. *Wang Chun et al.*[Error! Reference source not found.] used the untractless Kalman filter method to measure the SOC of supercapacitors, and adopted the symmetric sampling method. SOC is estimated by observing the terminal voltage of the capacitor, but this method will be interfered by some nonlinear factors such as battery parameters, so that the estimation errors are gradually superimposed. *Yang Qi et al.* [4] improved the traditional UKF by updating the ohm internal resistance of lithium battery online to improve the accuracy of battery parameters and reduce the influence of nonlinear factors on the algorithm. However, in the initial stage of this method, the error will gradually increase, reach a peak, and then slowly decrease, so it can only maintain a relatively high estimation accuracy in the later stage, so it has certain limitations for the accuracy of SOC research. *Zhao Yuehe et al.* [5] used UKF to estimate the health status of lithium batteries. Firstly, the state of charge of the battery and the internal resistance of the battery should be estimated in real time, and then the SOH should be calculated by using their arithmetic relationship.

With the continuous development of new energy technology, how to realize the joint estimation of SOC-SOH of lithium battery has also become a hot topic for scholars at home and abroad. *Ladpli P et al.*[6] used acoustic ultrasonic guided wave to monitor SOC and SOH of lithium-ion battery, and used a pressure plate sensor to install on the battery to realize the transmission and induction of guided wave. By observing the change of flight time and signal amplitude of guided wave, and using the relationship between it and electrochemical charge and discharge cycle and life, An analytical acoustic model was developed to simulate the changes of electrode modulus and density during cycling, and to verify the absolute value and range of the flight time of the experimental guided wave, so as to accurately estimate SOC and SOH. *Lai X et al.*[7]proposed to jointly estimate the SOC and SOH of lithium batteries by considering the influence of temperature factors, and combined the forgetting factor recursive least squares algorithm, total least squares algorithm and unscused Kalman filter algorithm. In the first step of this method, the least squares algorithm was used to identify and update the parameters of the equivalent circuit model in real time under different battery aging degrees. In the second step, the total least squares algorithm is used to estimate the battery SOH to improve the estimation accuracy of SOC. Finally, the unsculated Kalman filter algorithm is used to calculate the SOC of the battery, and then a more accurate SOH is obtained according to the SOC trajectory calculated by the algorithm. The algorithm is verified by experiments on circulating batteries. For temperature changes of up to 35 degrees Celsius and capacity attenuation of up to 10%, the joint estimation of SOH and SOC for lithium-ion batteries can achieve ultra-low errors of 2%.

Now, as lithium-ion batteries become more widely used, the feasibility of algorithms that estimate while ensuring real-time performance and accuracy is becoming increasingly important. *Wang Huile et al.*[9] used Thevenin equivalent circuit to fit the relationship between open circuit voltage and SOC, established a battery capacity model, and accurately predicted the changes of SOC and SOH during the dynamic operation of lithium-ion batteries through the theory of multi-time scale, and realized the joint estimation of SOC-SOH of lithium batteries on multi-time scale. By establishing a series of state equations, *Yin X et al.*[10] used the algorithm of unscused particle filter to realize the joint estimation of the two state quantities of lithium-ion battery in multiple times and degrees. According to the results of SOH estimation, the model parameters and capacity parameters of SOC estimation were updated, among which, The estimated value of the online health index is used as the observed quantity to realize the online joint estimation of SOC and SOH. *Zhang Xifeng et al.*[11] used adaptive extended Kalman particle filter to estimate SOC and SOH, and proposed to use the estimation results of SOH to revise SOC considering the deterioration characteristics of batteries. *Mo Yimin et al.*[12] adopted the improved double Kalman filter method, which did not need to rely too much on the accurate model and reduced the accumulated error caused by the ampere-hour integration method for current measurement.

With the continuous progress of the new energy industry, the accuracy of these estimation methods can no longer meet the needs of development to a certain extent. Therefore, scholars are constantly studying new methods to estimate the state of lithium batteries. *Moura SJ et al.*[15] mathematically modeled the battery by partial differential equation (PDE) and used adaptive PDE observer to estimate the state of the battery because the battery dynamics was constrained by the electrochemical principle. *Li Hanqi*[13] made a detailed study on the volume Kalman filter (CKF) algorithm and compared it with EKF and UKF, and the results showed that, In terms of estimation accuracy and robustness, CKF is better than EKF and UKF. *Li Gang et al.*[14] used the dual-volume Kalman filter (DCKF) to conduct in-depth estimation of vehicle state and road adhesion coefficient, and concluded that DCKF had higher estimation accuracy than DEKF. *Zhang Yuanjin et al.*[16] adopted firefly algorithm and proposed an improved Firefly optimization extended Kalman Filter (IFA-EKF) algorithm.

Most of the traditional SOC estimation algorithms are based on ampace-hour measurement method and

open-circuit voltage method, ignoring the influence of some environmental factors. For example, temperature change, load current, etc. The improvement of the algorithm is the difficulty of this study. In order to improve the accuracy of estimation and reduce the error rate of estimation, the algorithm is improved. In the process of experiment, it may be very difficult to design an improved algorithm independently. Therefore, according to the previous analysis of the traditional algorithm, we can learn from each other's strengths and make up for each other's weaknesses, and combine the traditional algorithm to achieve the improvement of the algorithm and achieve the expected results.

In order to make up for the shortcomings of the traditional algorithm, on the basis of selecting the appropriate battery model, this paper establishes the battery model, adopts the double extended Kalman filter method, the double particle filter method and the double volume Kalman filter method to jointly estimate the SOC-SOH of the lithium battery in two states, and analyzes the source of the error and the shortcomings of the algorithm. The double Kalman filter method is a relatively new estimation method, which is rarely used to study the state of batteries. The method of combining with the traditional algorithm is adopted to analyze and solve the shortcomings of the traditional algorithm, so as to reduce the error of the estimation results. Therefore, this paper will carry out the research of lithium ion battery charge state and health state estimation based on double Kalman filter algorithm and particle filter algorithm.

2 Lithium-ion batteries and SOC and SOH analysis

2.1 Lithium-ion battery performance

2.1.1 Comparison of different lithium batteries

The main structure of lithium-ion battery is generally composed of positive electrode material, negative electrode material, organic electrolyte and battery shell.

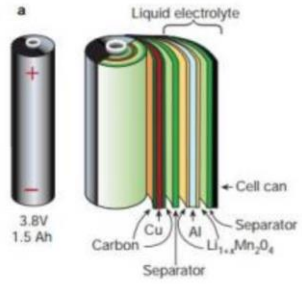

Figure 0-1 Structure diagram of cylindrical lithium battery[16]

According to the different cathode materials of lithium-ion batteries, they can be divided into: lithium cobaltate batteries, lithium manganate batteries, ternary lithium batteries and lithium iron phosphate batteries. Cathode materials account for 30% to 40% of the cost of lithium-ion batteries, which directly affects the performance of lithium-ion batteries. The following table lists the performance indicators of lithium-ion batteries with different cathode materials[18].

Table 0-1 Comparison of lithium ion properties of different cathode materials

Types of lithium batteries	Lithium cobalt acid	Lithium manganate	Three element material	Lithium iron phosphate
Electrode material	$LiCoO_2$	$LiMn_2O_4$	$LiCo_xNi_yMn_{1-x-y}O_2$	$LiFePO_4$
Safety performance	Low	Medium	Medium	Medium to high
Nature of pollution	Harmful	Harmless	Harmful	Harmless
Cost	Higher	Low	Higher	Low
Number of cycles	>500	>500	>1000	>2000
Density of energy	High	Medium	High	Medium
Resources of Materials	Cobalt deficiency	Rich	Cobalt deficiency	Cobalt deficiency

According to the above table compared with the other three materials of lithium batteries, it can be seen that lithium iron phosphate battery has no pollution, safe and environmental protection, does not contain toxic metal elements, and low cost, can be recycled more times, longer life. Therefore, compared with the other four kinds of lithium batteries, the lithium iron phosphate battery is the optimal choice and can be used as the research object of this paper.

2.1.2 Working principle of lithium iron phosphate battery

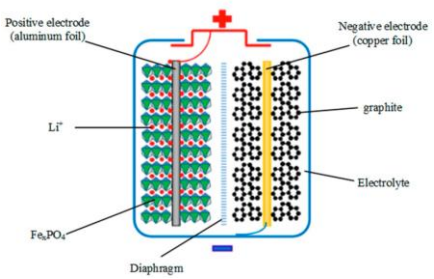

Figure 0-2 Internal structure diagram of lithium iron phosphate battery[37]

The internal structure of lithium iron phosphate battery is shown in the following figure[19]. It is the positive electrode material of lithium batteries and is directly connected to aluminum foil. The material of the negative electrode is directly connected to the copper material. The inside of the battery is filled with an organic electrolyte, and a diaphragm in the middle acts as a separation between the positive and negative electrodes. Electrons (e^-) cannot pass through the polymer diaphragm, but lithium ions (Li^+) can.

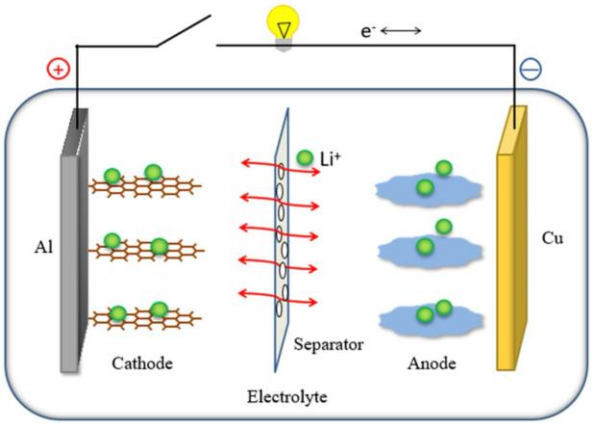

Figure 0-3 Schematic diagram of battery operation[39]

The above figure shows the working principle of lithium-ion battery[20]. During charging, lithium ions from the positive end of the battery will move through the diaphragm in the direction of the negative end. In the discharge process, the lithium ions present in the negative electrode will move through the polymer diaphragm in the direction of the positive electrode. Therefore, the mutual movement of lithium ions between the positive and negative materials inside the battery forms the circuit inside the battery. The chemical reaction equation of lithium iron phosphate battery is (2-1) ~ (2-8)[21].

The chemical equation for charging:

anode:

$$LiFePO_4 - xe^- = Li_{1-x}FePO_4 + xLi^+ \quad (2\text{-}1)$$

Cathode:

$$C_6 + xLi^+ + xe^- = Li_xC_6 \quad (2\text{-}2)$$

Battery reaction:

$$C_6 + LiFePO_4 = Li_xC_6 + Li_{1-x}FePO_4 \quad (2\text{-}3)$$

Chemical equations for discharge：

Negative electrode:

$$Li_xC_6 - xe^- = C_6 + xLi^+ \quad (2\text{-}4)$$

Positive electrode:

$$Li_{1-x}FePO_4 + xLi^+ + xe^- = LiFePO_4 \quad (2\text{-}5)$$

Battery reaction:

$$Li_xC_6 + Li_{1-x}FePO_4 = C_6 + LiFePO_4 \quad (2\text{-}6)$$

The above reaction can be simply written as follows:

Negative electrode:

$$Li - e^- = Li^+ \quad (2\text{-}7)$$

Positive electrode:

$$Li^+ + e^- = Li \quad (2\text{-}8)$$

2.2 SOC estimation method

2.2.1 Definition of SOC

SOC (state of charge) is the state of charge of the battery, which is used to represent the remaining battery power. The expression (2-9) is:

$$SOC(t) = \frac{Q_m(I) - Q_t(I)}{Q_m(I)} \quad (2\text{-}9)$$

where, $SOC_t(I)$ is the SOC value of the battery at time t, $Q_m(I)$ is the rated capacity of the battery, $Q_t(I)$ represents the amount of power discharged by the battery with current I in time t. SOC=1 means that the battery is fully charged and is fully charged; SOC=0 indicates that the battery has been completely discharged.

2.2.2 Common estimation methods for SOC

1. Ampere integral method

By integrating the current over a period of time, the amount of power released by the battery can be obtained, and the current value can be obtained by combining the initial SOC value of the lithium battery[22]. The expression (2-10) can be obtained by the Ampere-hour integration method:

$$SOC_{k+1} = SOC_k + \int_0^t \frac{\eta \cdot i}{C_t} dt \quad (2\text{-}10)$$

SOC_{k+1} is the SOC value of the lithium-ion battery at the time k+1. η is the charging and discharging efficiency of the battery, which is 1 in most cases; Ct is the rated capacity of the battery.

Although this method is simple and practical, it can only calculate the change of SOC, and cannot determine the actual value of SOC without knowing the initial value. Moreover, there is no feedback correction link, which leads to the accumulation of estimation error and the constant deviation between SOC estimation results and the actual situation, which is a problem.

2. Kalman filter algorithm

Kalman filter algorithm is the most widely used algorithm to estimate the state of charge of lithium-ion battery. Kalman filter is an adaptive filter, which takes the control input and observation value of the estimated object as input, and realizes the optimal estimation in the sense of the minimum error variance of the state variable of the estimated object dynamic process and the observed output[23].

The Kalman filter algorithm is not difficult to calculate and can be easily applied in engineering. Its disadvantage is that it is only applicable to linear systems, and applying it directly to highly nonlinear systems, such as batteries, will lead to large errors in the results.

3. Estimation methods used in this paper
In order to solve a series of problems caused by nonlinear systems, many researchers have proposed nonlinear Kalman filtering algorithms. For example, Extended Kalman filter (EKF) plays an important role in solving this problem.

The nonlinear Kalman filter algorithm can be roughly regarded as a linear system problem, and is handled by the traditional Kalman filter algorithm principle. However, the new nonlinear Kalman filter algorithm can update the data in real time, which can ensure the accuracy of the estimation. Compared with other estimation methods, the nonlinear Kalman filter algorithm ensures the accuracy of SOC estimation. In the fourth section, the nonlinear Kalman filter algorithm and particle filter algorithm are analyzed in detail.

2.3 The estimation method of SOH

2.3.1 Definition of SOH

SOH (state of health) refers to the health state of the battery, and the capacity is selected as the state variable to estimate SOH, which is defined as the percentage of the maximum capacity that can be charged or discharged of the lithium-ion power battery to its rated capacity under certain conditions, and its expression is (2-10) :

$$SOH_Q = \frac{Q_{now}}{Q_{start}} \qquad (2\text{-}10)$$

The largest available capacity of the Q_{now} battery; Rated capacity of the Q_{start} battery.

2.3.2 Common estimation methods for SOH

According to the current research progress, the common methods for battery health state estimation can be divided into four categories[24].

1. Direct measurement method
The direct discharge method, the most direct way to measure the SOH of the lithium battery is to let the single battery actually discharge once and measure the amount of power released. It is a more reliable method to measure and estimate the health state of the battery by using the load. However, there are also some disadvantages such as capacitance/energy measurement and internal ohmic resistance measurement, which are very complex to implement, need to test the battery parameters offline, and can not be monitored in real time online.

2. Indirect analysis method
The internal resistance method does not directly measure the capacity of the battery, but estimates the relationship between the internal resistance and the battery health state. However, this method is difficult to estimate, and the internal resistance requirements of the battery are more tricky, generally at the milliohm level, and it is difficult to measure the internal resistance of the battery. Therefore, this method has not been widely used.

3. Data-driven approach
The SOH of lithium-ion batteries is predicted by using historical data, that is, the key aging information of historical data[26] extracted by a specific learning algorithm.

4. Model method
Some adaptive techniques known in control theory are used to connect the physical model of the battery with the battery parameters to predict the battery health state[25]. This approach requires careful analysis of the chemical reactions that take place inside the battery to build a model and use that model to calculate changes in battery capacity.

5. the method used in this paper
SOH is determined by the relationship between ohmic internal resistance and SOH, so the ohmic internal resistance is regarded as a slowly changing system state. In this paper, the battery internal resistance R_0 is taken as the characteristic quantity of SOH, and the following is obtained:

$$R_{0,k+1} = R_{0,k} + r_k \qquad (2\text{-}11)$$

$$V_{T,k} = V_{OC}(SOC_k) - R_{0,k}I_k - V_{C1,k} + n_k \qquad (2\text{-}12)$$

$$SOH = \frac{R_{0_{EOL}} - R_{0_{Current}}}{R_{0_{EOL}} - R_{0_{New}}} \times 100\% \qquad (2\text{-}13)$$

where R_{EOL} -internal resistance at the end of battery life.

3 Battery model

3.1 Commonly used battery models

3.1.1 Electrochemical model

The lithium-ion electrochemical model is a simplification of the battery to a system consisting solely of positive and negative electrodes, separators, and organic electrolytes. According to the chemical reactions occurring inside the lithium battery, thermodynamic phenomena to establish the model. The electrochemical model has very important physical significance. This model takes into account the parameters such as the structure and constituent materials of the battery, and can accurately express the working principle and chemical reaction of the lithium-ion battery. However, the internal changes of the battery, physical changes and chemical changes continue to appear, resulting in the use of such models to calculate more difficult, can not be used in practical work.

1. P2D model
P2D (Pseudo Two Dimensional Model) is a classical

pseudo two dimensional electrochemical model of lithium-ion battery proposed by Newman and Doyle. This model can describe the internal dynamic behavior of the battery, and has the advantages of accurate model and high calculation accuracy[27]. The following figure shows the schematic diagram of P2D model of lithium-ion battery[28]. The P2D model needs to calculate the concentration of lithium ions, the solid phase potential, and the liquid phase potential through five equations to simulate the actual performance of lithium ion batteries.

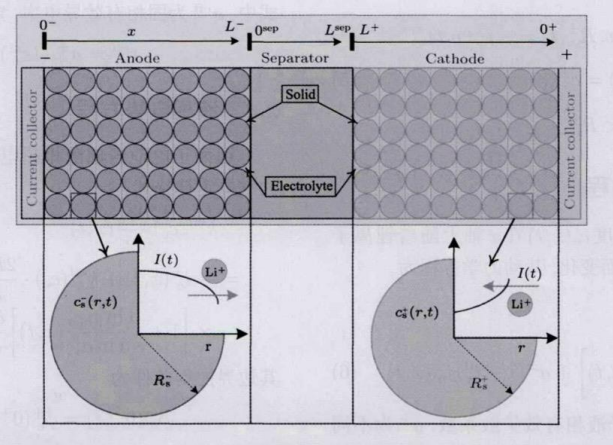

Figure 0-1 Schematic diagram of the P2D model of the Li-ion battery[27]

2. SP2D model

Due to the complexity of the traditional pseudo-two-dimensional electrochemical model, the computational efficiency is extremely low. The SP2D model is a simplification of the P2D model. By simplifying the solid phase and liquid phase modules of the lithium battery model, the dimensions of the cathode and anode diffusion equations are reduced, and the computational complexity is greatly reduced.

3. Shepherd model

The Shepherd model, proposed by C.M. Shepherd in 1965, is a model that describes the electrochemical state of a battery according to its voltage and current based on its electrochemical behavior [29]. The electrochemical model equation is (3-1) :

$$U = U_{OC} - R_0 I - \frac{R_1}{SOC} \qquad (3\text{-}1)$$

3.1.2 Equivalent circuit model

The equivalent circuit model of lithium battery is to avoid the study of too complex electrochemical internal reactions, only using voltage sources, resistors, capacitors and other often practical electrical components, to simulate the charging and discharging reaction of lithium battery, this model is the most commonly used lithium battery model in the study. Common equivalent circuit models include Rint model, RC model, Thevenin model, PNGV model, etc.

1. Rint model

The Rint model is also an internal resistance model, and the structure of the circuit is shown in Figure 3-2. The internal resistance model is an ideal voltage source connected in series with a resistor. The equation for the relationship between voltage and current is (3-2) :

$$U_0 = U_{OC} - I_L R_k \qquad (3\text{-}2)$$

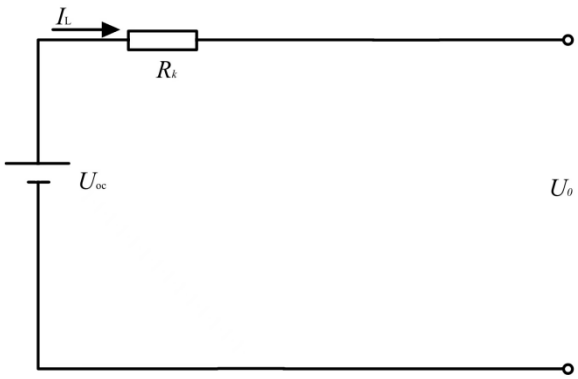

Figure 0-2 The Rint model

2. Thevenin model

The Thevenin model is also known as the first-order RC model, and the circuit structure is shown in Figure 3-3. The main principle is to add a RC parallel circuit on the basis of the Rint equivalent circuit model, RC parallel circuit to simulate the dynamic process of the battery. The equation for the relationship between voltage and current is (3-3) - (3-4) :

$$U_C = -\frac{U_C}{R_p C_p} + I_L R_0 \qquad (3\text{-}3)$$

$$U_0 = U_{OC} - U_C - I_L R_0 \qquad (3\text{-}4)$$

3. PNGV model

The PNGV equivalent circuit model was proposed by the United States New Generation Vehicle Cooperation Program in 2001, and its structure is shown in Figures 3-4. Based on Thevenin's model, this model adds a capacitor to express that with the increase of time, the voltage changes due to the accumulation of current, and the response accuracy will not be affected by the dynamic change of the state of charge [30]. The equation of state is (3-5) :

$$\begin{pmatrix} \dot{U}_b \\ \dot{U}_{cp} \end{pmatrix} = \begin{pmatrix} -\frac{1}{C_p * R_p} & 0 \\ 0 & 0 \end{pmatrix} \begin{pmatrix} U_b \\ U_{cp} \end{pmatrix} + \begin{pmatrix} -\frac{1}{C_b} \\ -\frac{1}{C_p} \end{pmatrix} u \qquad (3\text{-}5)$$

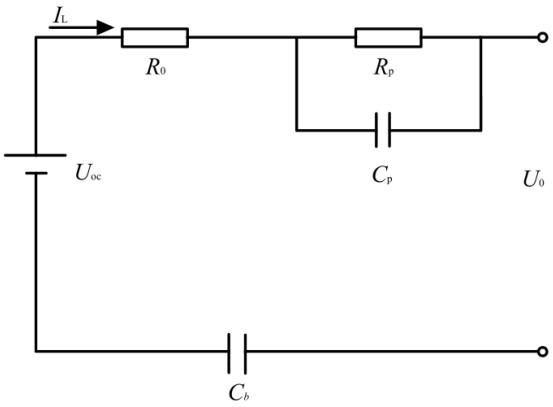

图 0-3 PNGV model

3.2 Selection of battery

After the above analysis, it can be concluded that the electrochemical model is not easy to realize because of too many parameters to be considered and the complex calculation process. Rint equivalent circuit model only consists of a voltage source and a resistor, the structure will be too simple, the accuracy of calculation is not high, and there is a large error with the actual work of lithium-ion battery. PNGV equivalent circuit model can be calculated accurately, but the process of getting model parameters is very complex. At present, Thevenin equivalent circuit model is mainly used to estimate the SOC of lithium-ion battery. The model consists of an RC circuit and a pulse equivalent circuit. The RC circuit measures the amount of electricity from the current, while the pulse equivalent circuit measures the voltage. Although the model is simple and easy to obtain, has fewer parameters and is simple and fast to calculate, it can not accurately reflect the actual characteristics of the battery in the actual use process because it only considers the current change during a single charge and discharge and the influence of temperature on the charging and discharging characteristics during the charging and discharging process. Moreover, the pulse equivalent circuit model does not take into account the nonlinear attenuation effect of current in the second-order RC circuit and the different effects of temperature on charge and discharge characteristics, which leads to errors.

Therefore, after considering the advantages and disadvantages of the above different battery models, the stability of the model should also be considered, and the dynamic characteristics of the battery can be well described. In more complex working conditions, a lot of calculation can be avoided. So this paper will use Thevenin model with moderate difficulty and easy to obtain parameters. However, the first-order Thevenin equivalent circuit model cannot well simulate the polarization reaction occurring in the working state of the battery. Therefore, in order to improve the accuracy of the model, a RC parallel circuit will be added to the model. The structure of the improved lithium battery model is shown in Figure 3-5:

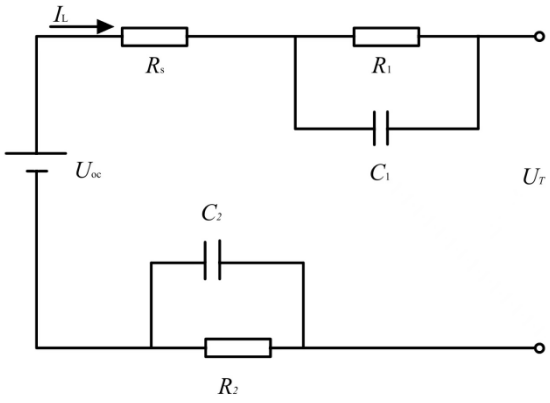

Figure 0-4 The second-order Thevenin model

The equation of state is (3-6) :

$$\begin{pmatrix} U_1 \\ U_2 \end{pmatrix} = \begin{pmatrix} -\frac{1}{R_1C_1} & 0 \\ 0 & -\frac{1}{R_2C_2} \end{pmatrix} \begin{pmatrix} U_1 \\ U_2 \end{pmatrix} + \begin{pmatrix} \frac{1}{C_1} \\ \frac{1}{C_2} \end{pmatrix} I_L \qquad (3\text{-}6)$$

Relation expression of circuit model:

With KVL's law, it follows that (3-7) :

$$U_T = U_{oc}(SOC) - R_0 I - U_{C1} - U_{C2} \qquad (3\text{-}7)$$

According to KCL, each RC loop has the following relations (3-8) to (3-9) :

$$\frac{dU_{C1}}{dt} = \left(\frac{1}{C_1}\right) I - \left(-\frac{1}{R_1C_1}\right) U_{C1} \qquad (3\text{-}8)$$

$$\frac{dU_{C2}}{dt} = \left(\frac{1}{C_2}\right) I - \left(-\frac{1}{R_2C_2}\right) U_{C2} \qquad (3\text{-}9)$$

It is discretized and integrated into the form of space state equation (3-10) - (3-11) :

$$\begin{pmatrix} SOC_{k+1} \\ U_{C1,k+1} \\ U_{C2,k+1} \end{pmatrix} = \begin{pmatrix} 1 & 0 & 0 \\ 0 & e^{\left(-\frac{T}{R_1C_1}\right)} & 0 \\ 0 & 0 & e^{\left(-\frac{T}{R_2C_2}\right)} \end{pmatrix} \begin{pmatrix} SOC_k \\ U_{C1,k} \\ U_{C2,k} \end{pmatrix} + \begin{pmatrix} \left(-\frac{T}{C_{bat}}\right) \\ R_1\left(1 - e^{\left(-\frac{T}{R_1C_1}\right)}\right) \\ R_2\left(1 - e^{\left(-\frac{T}{R_2C_2}\right)}\right) \end{pmatrix} I_k + w_k \qquad (3\text{-}10)$$

$$U_{T,k} = U_{oc}(SOC_k) - R_0 I_k - U_{C1,k} - U_{C2,k} + v_k \qquad (3\text{-}11)$$

3.3 Battery model parameters

3.3.1 Open circuit voltage and SOC-OCV curve acquisition

The use of the second-order Thevenin equivalent circuit has been established above as the experimental circuit in this paper. Therefore, it is necessary to identify the parameters of the components in the circuit. In this paper, the battery model (battery) in Simulink is used to simulate the real battery. The lithium iron phosphate battery is set up, the working condition is 25 degrees Celsius, the rated voltage is 3.3V, the rated capacity is 2.3Ah, and the simulation is completed.

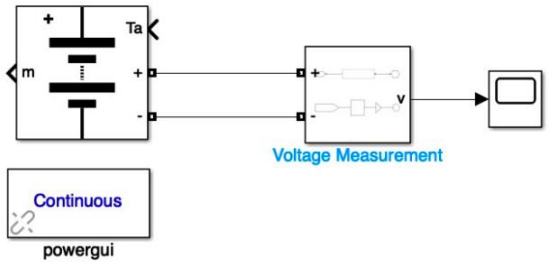

Figure 0-5 Simulation of open circuit voltage measurement circuit for lithium iron phosphate battery

The initial SOC value of the battery was modified to be 0.1, 0.2, 0.3, 0.4, 0.5, 0.6, 0.7, 0.8, 0.9, 1 respectively, and the corresponding open circuit voltage of the lithium battery was measured and recorded.

Table 0-1 Open circuit voltage identification results (unit: V)

SOC	OCV
0.1	3.3490
0.2	3.3611
0.3	3.3644
0.4	3.3656
0.5	3.3663
0.6	3.3668
0.7	3.3672
0.8	3.3674
0.9	3.3684
1.0	3.7480

Use Matlab to edit a script to plot the relationship between SOC and OCV, as shown in Figure 3-7, so that the mapping between the two can be established:

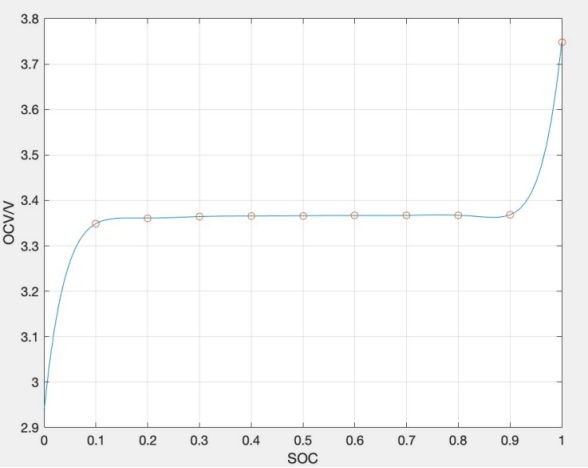

Figure 0-6 Relationship between OCV and SOC at 25 ° C

It can be seen from Figure 3-7 that when the lithium-ion battery is in the discharge state, the open circuit voltage of the battery will decrease with the continuous decrease of SOC. When SOC is reduced to 0.4, the drop range of the open circuit voltage becomes larger and the drop rate becomes larger. This is because in this interval of SOC, the battery is in the stage of excessive discharge, and the internal resistance value changes significantly[31], so the open circuit voltage changes significantly.

3.3.2 Parameter identification test

In this paper, the off-line recursive least squares method (FFRLS) is used to identify the model parameters and forget the factor. By minimizing the squared error and using the most appropriate function to query the data, the sum of the squared errors between the computed data and the actual value is minimized.

1. Internal resistance R_0 parameter identification results

Table 0-2 Identification result of R_0

SOC	R_0（Ω）
0.1	0.03243
0.2	0.05636
0.3	0.06592
0.4	0.06932
0.5	0.07032
0.6	0.07049
0.7	0.07037
0.8	0.07021
0.9	0.07042
1.0	0.07054

2. Identification of battery polarization impedance

Table 0-3 Results of cell polarization impedance identification

SOC	R_1（Ω）	R_2（Ω）	C_1（F）	C_2（F）
0.1	122.000	0.09727	1477.0	147.6
0.2	39.55000	0.20450	1367.0	696.7
0.3	11.15000	0.14360	2069.0	18.82
0.4	2.394000	0.12560	1374.0	18.82
0.5	0.106100	0.07958	1360.0	332.2
0.6	0.273600	0.02721	1768.0	218.0
0.7	0.192400	0.007575	1796.0	165.4
0.8	0.001819	0.02710	128.80	1123
0.9	0.002197	0.1885	161.20	1509
1.0	0.002183	0.4349	201.40	1634

According to Tables 3-1 to 3-3, it can be concluded that the battery model identification results are the same as those of reference[32], so the initial value of SOC is chosen as 0.8 in this paper, and the initial values of other parameters are shown in Tables 3-4 below:

Table 0-4 Initial parameter value selection

Parameters	Take a value
Initial capacity $C_0(Ah)$	**2.3**
Initial $R_0(\Omega)$	**0.07021**
Initial $R_1(\Omega)$	**0.001819**
Initial $R_2(\Omega)$	**0.02710**
Initial $C_1(F)$	**128.8**
Initial $C_2(F)$	**1123.0**

4 Joint SOC-SOH estimation for lithium batteries

As various methods have been analyzed to estimate the charging state and health state of lithium-ion batteries, it can be known that the Kalman filter method can obtain the state information we need. It is a recursive estimation algorithm, which can monitor the state quantity in real time, and can describe the actual feedback state and model parameters. KF algorithm has high accuracy and low computational difficulty compared with other estimation methods, so it is more suitable for studying the state of lithium batteries and has a wider application field.

Lithium battery is a nonlinear system, so the traditional Kalman filter method can not accurately estimate the state of the battery, so scholars at home and abroad have studied the nonlinear Kalman filter algorithm. At present, the two most common algorithms are the unscent-Kalman filter algorithm and the extended Kalman filter algorithm. In this paper, the double Kalman filter algorithm and the particle filter algorithm are used to jointly estimate the SOC and SOH of lithium-ion batteries.

4.1 Double extended Kalman Filter (DEKF)

The Dual Extended Kalman Filter (DEKF) algorithm uses two independent filters to estimate the parameters and charge states of lithium-ion batteries, monitors and updates the model parameters in real time based on the original parameters, and uses the updated model parameters to improve the SOC rating.

1、SOC estimation principle (first EKF filter) :

$$x_k = \left(SOC_k, U_{C1,k}, U_{C2,k}\right)^T \quad (4\text{-}1)$$

According to 3-10 and 3-11, the state of battery charge and the observation equations (4-2)~(4-3) can be obtained:

$$x_{k+1} = f(x_k, U_k) + w_k{}^x \quad (4\text{-}2)$$

$$y_k = g(x_k, U_k) + v_k{}^x \quad (4\text{-}3)$$

Where the output: $y_k = U_{0,k}$, Control variables: $U_k = I_k$, The process and observation noise are: $w_k{}^x \sim N(0, Q^x), v_k{}^x \sim N(0, R^x)$.

After the state of charge of the battery is estimated, SOC becomes the input quantity that has been determined. The state equation of θ and the observation equation (4-4) ~ (4-5) can be obtained from (4-2) ~ (4-3) :

$$\theta_{k+1} = \theta_k + w_k{}^\theta \quad (4\text{-}4)$$

$$y_k = g(x_k, u_k, \theta_k) + v_k{}^\theta \quad (4\text{-}5)$$

Where $\theta_k = [R_0, R_C, C_C, R_d, C_d]^T$, The process noise and the observation noise are respectively: $w_k{}^\theta \sim N(0, Q^\theta)$、$v_k{}^\theta \sim N(0, R^\theta)$.

The process of DEKF algorithm estimation:

First, initialize the parameters.

The second step is to update the parameters of the model over time: (4-6) ~ (4-7) :

$$\widehat{\theta_{k+1}}^- = \widehat{\theta_k}^+ \quad (4\text{-}6)$$

$$P_{\theta,k+1}{}^- = P_{\theta,k}{}^+ + Q_k{}^\theta \quad (4\text{-}7)$$

The third step needs to update the time state (4-8) to (4-9) :

$$\widehat{x_{k+1}}^{-} = f\left(\widehat{x_k}^{+}, u_k, \widehat{\theta_{k+1}}^{-}\right) \quad (4\text{-}8)$$

$$P_{x,k+1}^{-} = \widehat{A_k} P_{x,K}^{+} \widehat{A_i}^{T} + Q_i^{+} (4\text{-}9)$$

Step 4 Observe and predict states (4-10) - (4-12) :

$$K_k^x = P_{x,k+1}^{-} \widehat{H}_k^{xT} \left(\widehat{H}_k^x P_{x,k+1}^{-} \left(\widehat{H}_k^x\right)^T + R_k^x\right)^{-1}$$

(4-10)

$$\widehat{x_{k+1}}^{+} = \widehat{x_{k+1}}^{-} + K_k^x (y_k - \hat{y}_k)$$

(4-11)

$$P_{x,k+1}^{+} = \left(I - K_k^x \widehat{H}_k^x\right) P_{x,k+1}^{-}$$

(4-12)

The fifth step is matching covariance (4-13) to (4-15) :

$$B_k = \sum_{i=k+1}^{k} (y_k - \hat{y}_k)_i (y_k - \hat{y}_k)^T_i$$

(4-13)

$$Q_{k+1}^x = K_k^x B_k (K_k^x)^T$$

(4-14)

$$R_{k+1}^x = B_k - \widehat{H}_k^x P_{x,k+1}^{-} \left(\widehat{H}_k^x\right)^T$$

(4-15)

The sixth step is to observe and monitor the parameters of the model (4-16) to (4-18) :

$$K_k^\theta = P_{x,k+1}^{-} \left(\widehat{H}_k^\theta\right)^T \left(\widehat{H}_k^\theta P_{\theta,k+1}^{-} \left(\widehat{H}_k^\theta\right)^T + R^\theta\right)^{-1}$$

(4-16)

The above equation expression, updating the time state in real time, and also updating the observation of the state, can estimate the real-time model parameters and charge states

2. The estimation principle of SOH (second EKF filter) :

Since there is a certain relationship between the ohmic internal resistance and the health state of the lithium battery, therefore, the SOH can be determined according to this relationship. Considering the ohmic internal resistance as a slowly changing system state, the state equations (4-17) ~ (4-19) are obtained:

$$R_{0,k+1} = R_{0,k} + r_k$$

(4-17)

$$U_{T,k} = U_{oc}(SOC_k) - R_{0,k} I_k - U_{C1,k} - U_{C2,k} + n_k$$

(4-18)

$$SOH = \frac{R_{0_{EOL}} - R_{0_{Current}}}{R_{0_{EOL}} - R_{0_{New}}} \times 100\%$$

(4-19)

4.2 Dual Particle Filter (DPF)

The Dual Particle Filter (DKF) algorithm is a good nonlinear filtering method that is gradually emerging. Its basic principle is to use random samples in the space state to approximate the posterior probability density function, and estimate the state equation according to the Monte Carlo estimation method[35]. The double particle filter algorithm is used to estimate the SOC of lithium ion battery through two particle filters PF1 and PF2, PF1. PF2 estimates the internal resistance R_0 of lithium ion battery, and estimates the value of SOH through the relationship with SOH.

First, Equations 4-20 describe the posterior probability distribution at time k:

$$\left\{x_{0\,k}^i, w_k^i\right\}_{i=1}^{N_s}$$

(4-20)

$$p(x_{0\,k}|y_{1\,k}); \left\{x_{0\,k}^i, i = 0, \cdots, N_s\right\}$$

(4-21)

$$\left\{w_k^i, i = 0, \cdots, N_s\right\}$$

(4-22)

$$x_{0\,k} = \{x_i, i = 0, \cdots, k\}$$

(4-23)

Where Equation 4-21 is the particle set with weight of equation 4-22, and equation 4-23 is the state set at each time from 0 to k. Finally, normalizing all the weights can obtain the posterior probability distribution of the target state, and the discrete weighted value is equation 4-2:

$$p(x_{0\,k}|y_{1\,k}) \approx \sum_{i=1}^{N_s} w_k^i \sigma(x_{0\,k} - x'_{0\,k}) \quad (4\text{-}24)$$

If the particle set can be obtained by analyzing the important density function 4-25, then the weights can be written as 4-26:

$$q\left(x_{0\,k}^i | y_{1\,k}\right)$$

(4-25)

$$w_k^i \propto \frac{p\left(x_{0\,k}^i | y_{1\,k}\right)}{q\left(x_{0\,k}^i | y_{1\,k}\right)}$$

(4-26)

The importance density can be decomposed into 4-27:

$$p(x_{0\,k}|y_{1\,k}) = \frac{p(y_k|x_{0\,k}, y_{1\,k})p(x_{0\,k}|y_{1\,k-1})}{p(y_k|y_{1\,k-1})} = \frac{p(y_k|x_k)p(x_k|x_{k-1})}{p(y_k|y_{1\,k-1})}p(x_{0\,k-1}|y_{1\,k-1})$$

$$\propto p(y_k|x_k)p(x_k|x_{k-1})p(x_{0\,k-1}|y_{1\,k-1}) \quad (4\text{-}28)$$

According to equations (4-26) to (4-28), we can obtain the importance equations 4-29:

$$w_k^i = w_{k-1}^i \frac{p(y_k|x_k^i|x_{k-1}^i)}{q(x_k^i|x_{0\,k-1}^i, y_{1\,k})}$$

(4-29)

If $q(x_k^i|x_{0\,k-1}^i, y_{1\,k}) = q(x_k|y_{k-1}, y_k)$, The important density function is only determined by x_{k-1} and y_k, Therefore, the modified weights will become 4-30:

$$w_k^i = w_{k-1}^i \frac{p(y_k|x_k^i)p(x_k^i|x_{k-1}^i)}{q(x_k^i|x_{k-1}^i, y_k)}$$

(4-30)

Normalization of weights can obtain Eqs. 4-31:

$$w_k^i = \frac{w_k^i}{\sum_{i=1}^{N_s} w_k^i}$$

(4-31)

The posterior probability density is given by Eqs. 4-32:

$$p(x_k|y_{1\,k}) = \sum_{i=1}^{N_s} w_k^i \sigma(x_k - x_k')$$

(4-32)

4.3 Dual Volume Kalman Filter (DCKF)

The Cubature Kalman Filter (CKF) algorithm based on the third-order spherical diameter volume criterion was formally proposed by Dr. Arasaratnam and Professor Haykin et al. in 2009[35]. The principle of the volume Kalman filter (CKF) algorithm is to select a set of volume points according to the radial volume reference of the third degree sphere, make the volume points approximate to the nonlinear function, and calculate the inverse mean and error covariance of the nonlinear function transmission. The double volume Kalman filter method calculates the volume points twice, brings the first calculated volume points into the nonlinear state equation for state prediction, and then predicts the covariance. After that, it calculates the volume points for the second time, calculates the gain matrix, and updates the state prediction and covariance to obtain the SOC estimate of the lithium-ion battery.

$$q(x_{0\,k}^i|y_{1\,k}) = q(x_k|x_{0\,k-1}|y_{1\,k})q(x_{0\,k-1}|y_{1\,k-1}) \quad (4\text{-}27)$$

The posterior probability density can be written as 4-28:

1. The third-order spherical radial volume criterion Integration for a Gaussian nonlinear function:

$$I(f) = \int_{R^n} f(x) \exp(-x^T x)dx$$

（4-33）

Where, is the nonlinear function, is the integral sought, is the dimensional integral domain, and is the state vector.

First, transform Eq. 4-31 into the spherical radial integral form, and then transform the state vector x in the Cartesian coordinate system into the radius r and the direction vector y, therefore, $x = ry, y^T y = 1, r \in [0, +\infty)$, thus,$x^T x = r^2$. Thus, the Gaussian integral 4-31 can be expressed as the following double integral:

$$I(f) = \int_0^{+\infty} \int_{U_n} f(ry) r^{n-1} \exp(-r^2)d\sigma(y)dr$$

（4-34）

$$I(f) = \int_0^{+\infty} S(r) r^{n-1} \exp(-r^2)dr$$

（4-35）

$$S(r) = \int_{U_n} f(ry)d\sigma(y)$$

（4-36）

Where equations 4-35 to 4-36 are the radial integral and spherical integral forms of Equation 4-34, and equation 4-34 is the radial integral, and can be approximated by Gauss-Hermitian criterion of individual points m_r.

$$\int_0^{+\infty} S(r) r^{n-1} \exp(-r^2)dr = \sum_{i=1}^{m_r} a_i S(r_i)$$

（4-37）

$$\int_{U_n} f(ry)d\sigma(y) = \sum_{j=1}^{m_s} b_j f(ry_j)$$

（4-38）

Applying the spherical volume criterion of the points to approximate equation 4-35, we can obtain equations 4-37 ~ 4-38, where, a_i、b_j are the corresponding weights. Combining the two formulae simultaneously can obtain the following formula:

$$I(f) = \int_{R^n} f(x)\exp(-x^T x)dx = \sum_{j=1}^{m_s}\sum_{i=1}^{m_r} a_i b_j f(r_i y_j) \quad (4\text{-}39)$$

Eq. 4-39 is the spherical radial volume criterion formula of $(m_r \times m_s)$, For the third order spherical radial volume criterion, take $m_r = 1, m_s = 2n$, where n is the dimension of the state vector.

$$I_N(f) = \int_{R^n} f(x)N(x;0,I)dx \approx \sum_{j=1}^{m} \omega_j f(\xi_j) \quad (4\text{-}40)$$

Equations 4-40 are obtained by representing equations 4-39 as mean 0 and covariance as identity matrix, where m is the number of volume points and $\omega_j = \frac{1}{m}$ represents the corresponding weight of volume points, $\xi_j = \sqrt{\frac{m}{2}}[\delta]_j$ is the set of volume points and $[\delta]_j$ represents the JTH volume point, as shown in Equation 4-41:

$$[\delta] = \left\{\begin{pmatrix}1\\0\\\vdots\\0\end{pmatrix},\begin{pmatrix}0\\1\\\vdots\\0\end{pmatrix},\cdots,\begin{pmatrix}0\\0\\\vdots\\1\end{pmatrix},\begin{pmatrix}-1\\0\\\vdots\\0\end{pmatrix},\begin{pmatrix}0\\-1\\\vdots\\0\end{pmatrix},\cdots,\begin{pmatrix}0\\0\\\vdots\\-1\end{pmatrix}\right\} \quad (4\text{-}41)$$

2. volume Kalman algorithm steps

Initialize:

$$\bar{x}_0 = E[x_0] \quad (4\text{-}42)$$

$$P_0 = E[(x_0 - \bar{x}_0)(x_0 - \bar{x}_0)^T] \quad (4\text{-}43)$$

Calculate the volume point:

$$x_{k-1}^{(i)} = S_{k-1}\xi^{(i)} + \hat{x}_{k-1} \quad i = 1,2,\cdots,2n \quad (4\text{-}44)$$

Where, $S_{k-1} = chol(P_{k-1})$, $chol()$ represents the Cholesky decomposition of the matrix, that is $P_{k-1} = S_{k-1}{S_{k-1}}^T$, n represents the number of state variables and ξ represents a set of standard volume points, which is given by the following equation:

$$\xi^{(i)} = \begin{cases}\sqrt{n}[\delta]^{(i)} & i = 1,2,\cdots n\\ -\sqrt{n}[\delta]^{(i)} & i = n+1, n+2,\cdots 2n\end{cases} \quad (4\text{-}45)$$

where δ represents the identity matrix and i represents the column vector of i.

The volume points are propagated through the state space equation:

$$\chi_{k|k-1}^{(i)} = f\left(x_{k-1}^{(i)}, u_{k-1}\right) \quad (4\text{-}46)$$

State prediction:

$$\bar{x}_{k|k-1} = \frac{1}{2n}\sum_{i=1}^{2n}\chi_{k|k-1}^{(i)} \quad (4\text{-}47)$$

Error covariance prediction:

$$P_{k|k-1} = \frac{1}{2n}\sum_{i=1}^{2n}\left(\chi_{k|k-1}^{(i)} - \bar{x}_{k|k-1}\right)\left(\chi_{k|k-1}^{(i)} - \bar{x}_{k|k-1}\right)^T + Q_{k-1} \quad (4\text{-}48)$$

where Q_{k-1} is the process noise covariance matrix at the time step k−1.

The volume points are calculated according to the predicted results:

$$x_{k|k-1}^{(i)} = S_{k|k-1}\xi^{(i)} + \hat{x}_{k|k-1} i = 1,2,\cdots,2n \quad (4\text{-}49)$$

The volume points are propagated through the state space equation:

$$z_{k|k-1}^{(i)} = g\left(x_{k|k-1}^{(i)}, u_k\right) \quad (4\text{-}50)$$

Measurement and prediction:

$$\bar{z}_{k|k-1} = \frac{1}{2n}\sum_{i=1}^{2n} z_{k|k-1}^{(i)} \quad (4\text{-}51)$$

Error covariance prediction:

$$P_{k|k-1}^{y} = \frac{1}{2n}\sum_{i=1}^{2n}\left(z_{k|k-1}^{(i)} - \bar{z}_{k|k-1}\right)\left(z_{k|k-1}^{(i)} - \bar{z}_{k|k-1}\right)^T + R_{k-1} \quad (4\text{-}52)$$

$$P_{k|k-1}^{xy} = \frac{1}{2n}\sum_{i=1}^{2n}\left(x_{k|k-1}^{(i)} - \bar{x}_{k|k-1}\right)\left(z_{k|k-1}^{(i)} - \bar{z}_{k|k-1}\right)^{T} \quad (4\text{-}53)$$

where, R_{k-1} is the measurement noise covariance matrix at the time step k−1.

Calculate the Kalman gain:

$$K_k = P_{k|k-1}^{xy}(P_{k|k-1}^{y})^{-1} \quad (4\text{-}54)$$

State estimation:

$$\hat{x}_k = \bar{x}_k - K_k(y_k - \bar{y}_k) \quad (4\text{-}55)$$

Update error covariance:

$$P_k = P_{k|k-1} - K_k P_{k|k-1}^{y} K_k^{T} \quad (4\text{-}56)$$

4.4 Validation of algorithm

In Chapter 3, the relational equations of the battery model are listed, and the SOC space state equations (3-10) ~ (3-11) are also listed. Moreover, the parameters R0, R1, R2, C1 and C2 used in the model have been given numerical values in Chapter 3.

According to the obtained experimental data, under the DST condition, the DEKF, DPF and DCKF algorithms are used to estimate the SOC and internal resistance R_0 of the lithium-ion battery, and then the results obtained by the estimation algorithm are compared with the simulation results. The results of the algorithm were evaluated by absolute error to verify the accuracy and stability of the algorithm.

4.4.1 Simulation results

Through the Matlab programming tool, the simulation program set the battery to discharge at 4A constant current, and the initial value of SOC was set to 0.8. The estimation effect of the algorithm under the constant discharge condition was compared.

1. Simulation results estimated by the double extended Kalman filter algorithm

The estimation results of SOC are shown in Figure 4-4, and the error of SOC estimation by DEKF algorithm is shown in Figure 4-5:

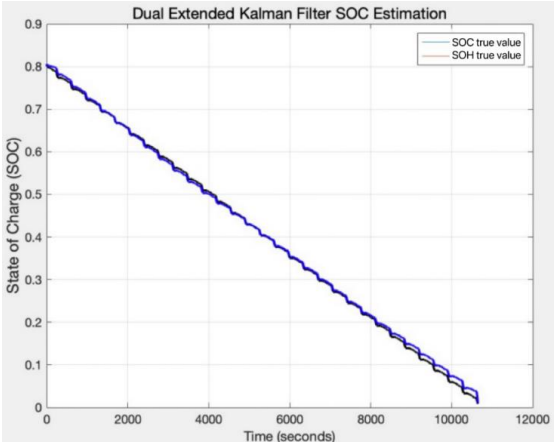

Figure4- 4 Diagram of SOC estimation results of DEKF algorithm

FIG. 4-4 shows that at the beginning of the experiment, within the entire range of SOC value from 0 to 100%, the change trend of SOC estimated value and the true value is similar. In a short period of time, the error value of SOC is close to 0, but with the increase of time, the estimated value of SOC gradually deviates from the true value.

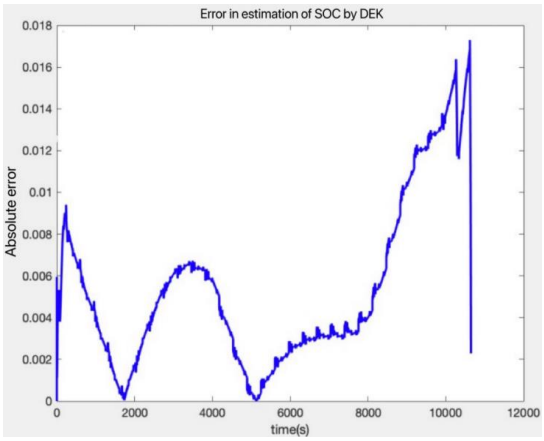

Figure 4- 5 Estimation error of SOC estimated by DEKF

Table 0-1 Error comparison of DEKF algorithm

Maximum absolute error	Mean absolute error	Median absolute error	Standard deviation of absolute error
1.73%	0.5391%	0.4129%	0.3939%

As can be seen from Table 4-1, when the DEKF algorithm is used to estimate SOC, the maximum absolute error is 1.73%, and the average absolute error is 0.5391%. Figure 4-6 depicts the curve of internal resistance R_0 with time:

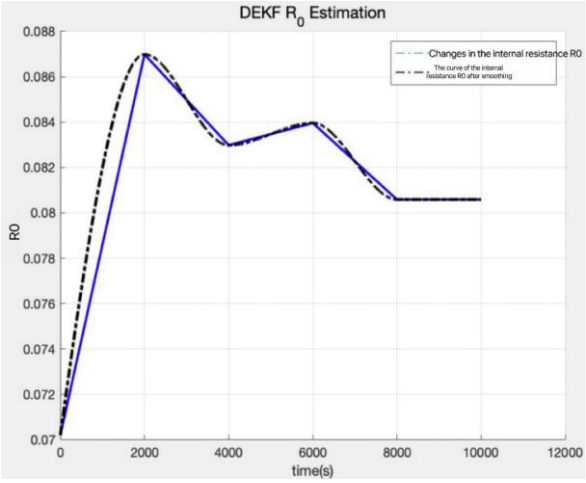

Figure 4- 6 The estimated curve of the internal resistance R_0 of the DEKF algorithm

If the ohmic internal resistance is set as a slowly changing system state parameter, the state of SOH can be determined by the change of internal resistance R_0 shown in FIG. 4-6. When the experiment reaches 1968s, the internal resistance R_0 reaches the maximum value of 0.08699 ohms, and stabilizes at 0.08059 ohms before the end of the experiment.

According to the estimation curve of R_0, when the lithium battery is in the state of charging and discharging, the internal resistance of the battery will become very obvious. According to formula 2-13, the estimated curve of SOH can be obtained in Figure 4-7:

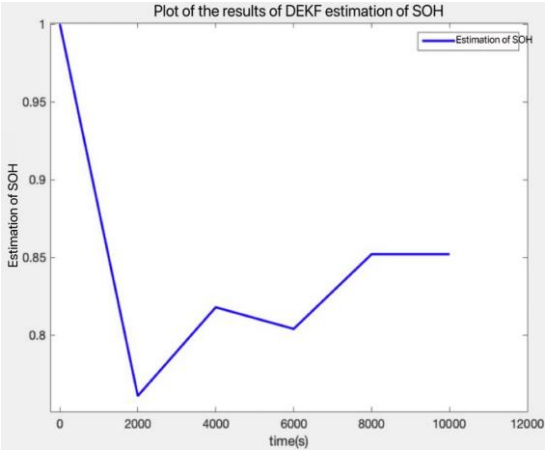

Figure 4- 7 Diagram of the DEKF algorithm SOH estimation results

The DEKF algorithm was used to estimate the SOH of lithium ion battery, which reached the minimum value of 76.0867% when the experiment was carried out in 2001 seconds, and stabilized at about 85% at the end of the experiment.

3. Simulation results estimated by the dual particle filter algorithm

In the m file program of Matlab, the number of particles is set to 200, the estimation results of SOC are shown in Figure 4-8, and the error of SOC estimation by DPF algorithm is shown in Figure 4-9:

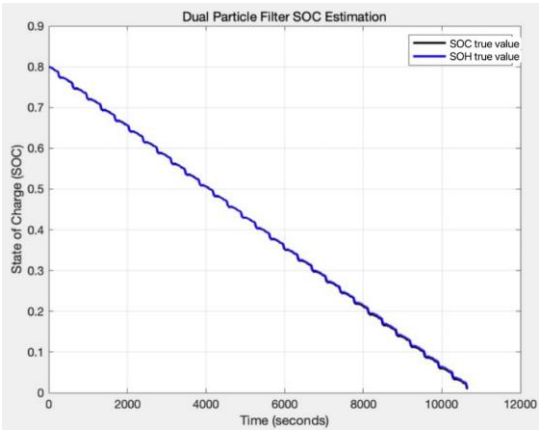

Figure 4-8 Diagrams of simulation results of SOC for DPF algorithm

It can be seen from Figure 4-8 that the change trend of SOC real value and estimated value is similar, while the estimated value of SOC is always under the real value curve, indicating that the calculation superposition of SOC of lithium-ion battery calculated by amp-time integration method has been out of the actual value of SOC estimation.

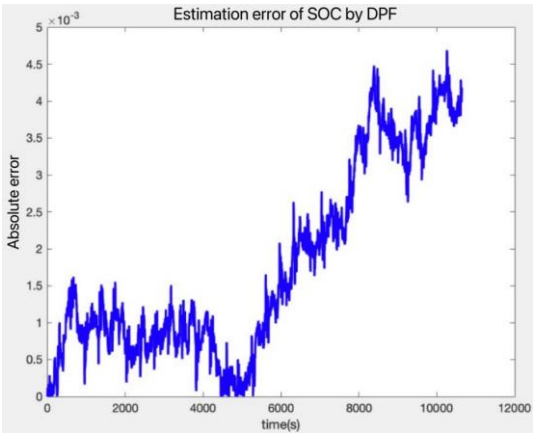

Figure 4- 9 Estimation error of SOC estimated by DPF

Table 0-2 Error comparison of DPF algorithm

Maximum absolute error	Mean absolute error	Median absolute error	Standard deviation of absolute error
0.4689%	0.1767%	0.1188%	0.1303%

As can be seen from Table 4-2, when the DPF algorithm is used to estimate SOC, the maximum absolute error reaches 0.4689%, and the average absolute error is 0.1767%. Figure 4-10 depicts the curve of internal resistance R0 with time, Figure 4-11 is the estimation curve of SOH of lithium ion battery:

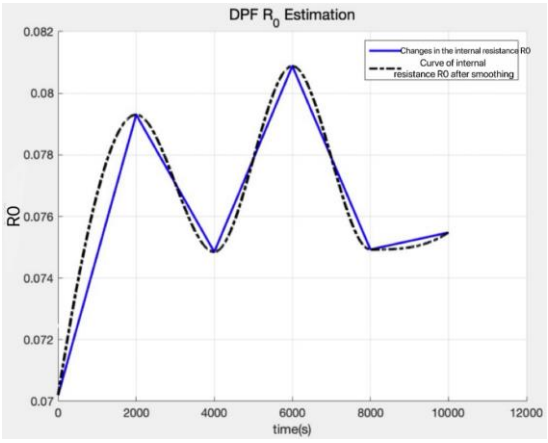

Figure 4- 10 The estimated curves of the internal resistance R_0 of the DPF algorithm

It can be seen from Figure 4-10 that the internal resistance R0 reaches a maximum value of 0.08087 ohms at 6048s of the experiment.

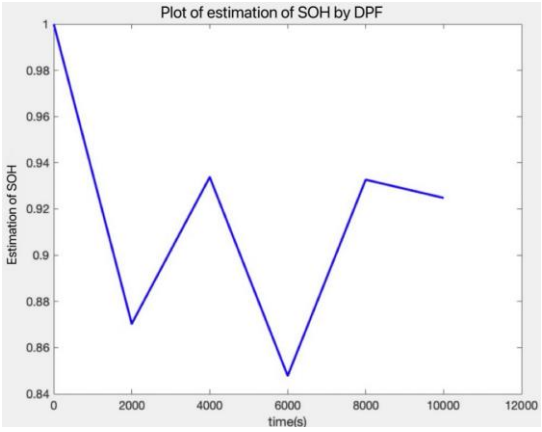

Figure 4- 11 SOH estimation results of DPF algorithm

The DPF algorithm was used to estimate the SOH, which reached the minimum value of 84.78% when the experiment was carried out for 6001s.

4. Simulation results estimated by dual-volume Kalman filter algorithm

The estimation results of SOC are shown in Figure 4-12, and the error of SOC estimation by DPF algorithm is shown in Figure 4-13:

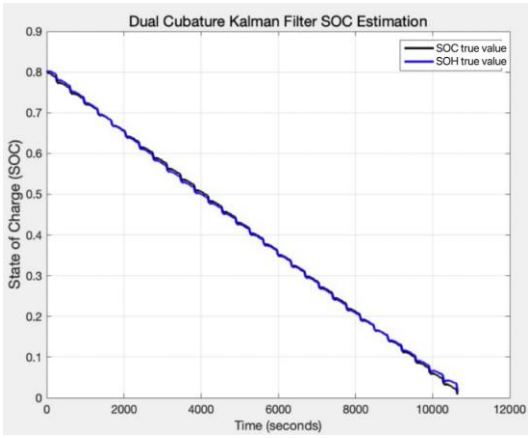

Figure 4- 12 Diagrams of SOC estimation results of DCKF algorithm

It can be seen from FIG. 4-12 that the real SOC value of the lithium-ion battery has a similar change trend to the actual value estimated by the algorithm, which indicates that the initial error of the estimated SOC value of the lithium-ion battery estimated by the dual-volume Kalman filter is small, but the error of the algorithm estimation results will gradually increase as the state of charge is estimated.

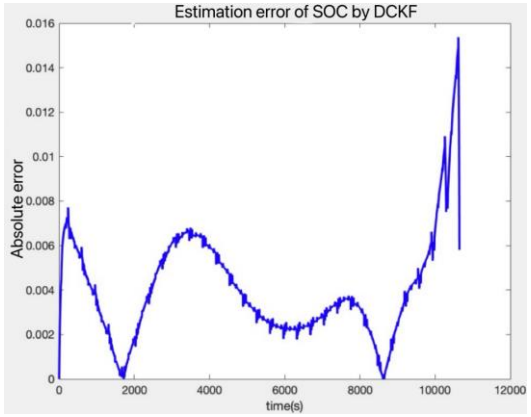

Figure 4- 13 DCEK estimates the estimation error of SOC

Table 0-3 Error comparison of DCKF algorithm

Maximum absolute error	Mean absolute error	Median absolute error	Standard deviation of absolute error
1.537%	0.4047%	0.3477%	0.2381%

As can be seen from Table 4-3, when the DCKF algorithm is used to estimate SOC, the maximum

absolute error reaches 1.537% and the average absolute error is 0.4047%. Figure 4-14 depicts the curve of internal resistance R_0 with time, Figure 4-15 is the estimation curve of SOH of lithium ion battery:

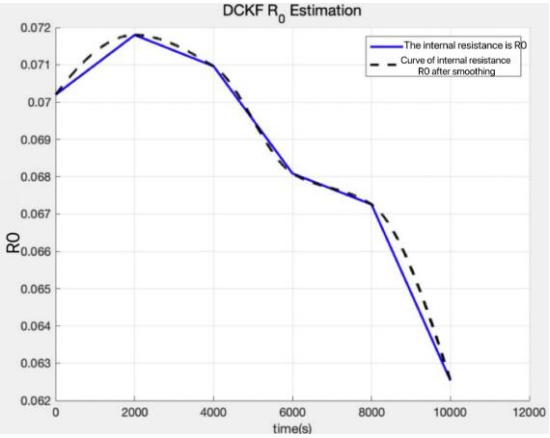

Figure 4- 14 Estimation curve of the internal resistance R_0 of the DCKF algorithm

According to Figure 4-14, when the experiment is carried out to 2019s, the internal resistance R_0 of the lithium-ion battery reaches the maximum value of 0.0718 ohms.

As shown in Figure 4-15, the SOH value of the lithium ion battery calculated by the DCKF algorithm will be greater than 100% after 5000s of the experiment, because the capacity regeneration of the lithium ion battery occurs in the process of charging[37].

4.4.2 Analysis of simulation results

By comparing the results of DEKF, DPF and DCKF algorithms for the joint simulation of SOC and SOH of lithium ion batteries, it can be seen that the DPF algorithm has the smallest error in the estimation of SOC, and its estimation effect is superior, which is significantly improved compared with DEKF and DCKF. Table 4-4 can visually observe and compare the errors of these three algorithms in estimation:

Table 0-4 Three algorithms estimate SOC result errors

Estimation by algorithm	Maximum absolute error	Mean absolute error	Median absolute error	Standard deviation of absolute error
DEKF	1.73%	0.5391%	0.4129%	0.3939%
DCKF	1.537%	0.4047%	0.3477%	0.2381%
DPF	0.4689%	0.1767%	0.1188%	0.1303%

It can be seen from Table 4-4 that under the three algorithms, the maximum error of the DPF algorithm remains within 1%, the average error remains within 1%, and the median absolute error remains within 1%, indicating that the performance of the DPF algorithm is superior, meets the accuracy and stability requirements of the lithium-ion battery state estimation, and has good robustness. It can provide certain reference value for practical application.

5 Conclusions and Prospects

5.1 Conclusion

In this paper, by analyzing the internal structure and working principle of lithium ion battery, the second-order Thevenin equivalent circuit model is selected as the battery model and its parameters are identified. In view of the shortcomings of the traditional algorithms, the DEKF, DPF and DCKF algorithms are selected to jointly estimate SOC and SOH, and the estimation results of these three algorithms are compared to further demonstrate the superiority of the algorithms. The main work completed is as follows:

Firstly, the types of lithium-ion batteries are introduced, and the background and significance of the research on the charge state estimation of lithium-ion batteries under the current social background are expounds. The common battery models on the market are compared and analyzed, some advantages of lithium iron phosphate batteries are summarized, the current research status at home and abroad is reviewed, and the feasibility of the algorithm is analyzed.

Several common battery models are analyzed, and the advantages and disadvantages of each model are summarized. Finally, the second-order Thevenin equivalent circuit model is selected as the research model in this paper to jointly estimate the SOC and SOH of lithium-ion batteries. The battery model in Simulink toolbox was used to calculate the open circuit voltage of the lithium iron phosphate battery under different SOC values, and the off-line recursive least squares method with forgetting factor (FFRLS) was used to identify the parameters of the lithium ion battery. According to the identification results, the model was verified by comparing with the relevant literature. The results show that the battery model selected in this paper can accurately describe the general variation law of the voltage at the two ends of the battery before and after the current pulse, and the identification results of the simulated voltage are consistent with those in the literature.

The principle of EKF, PF and CKF for SOC estimation

of lithium ion battery and the principle of DEKF, DPF and DCKF for SOC and SOH joint estimation are described, and the m file editing program code is used for simulation experiments in Matlab software to obtain the joint estimation results, and the estimation results of these three algorithms are compared and analyzed. The final experimental results show that compared with the other two algorithms, DPF performs better in terms of accuracy, stability and robustness when estimating the SOC of lithium ion batteries. The maximum error is less than 1%, which is 0.4689%. Moreover, DCKF will show the capacity regeneration when estimating the SOH of lithium ion batteries.

5.2 Future research

In this paper, the joint estimation algorithm of the state of charge and state of health of lithium-ion battery based on double Kalman filter is studied in detail, which plays a reference role in the future research on the development of new energy industry. However, due to the limitations of time and hardware conditions, there are still many aspects to be further strengthened, mainly the following suggestions:

The parameter identification method selected in this paper is offline identification, but the actual use of the battery is greatly affected by environmental conditions and operating conditions. The method of online parameter identification will be beneficial to further improve the estimation accuracy of the algorithm, so the research on the method of online parameter identification can be taken as the follow-up research direction.

With the continuous use of the battery, the number of charging and discharging cycles gradually increases, which will lead to certain problems in the battery, such as battery aging. Aging factors should then be added to the analysis of battery characteristics.

Reference

1. P. An and Q. Lu, "Application and development of lithium-ion secondary batteries," Journal of Peking University (Natural Science Edition), no. S1, pp. 1-7, 2006.
2. Q. Zhang, L. Zhang, and L. Dong, "Research on health evaluation of lithium power batteries based on dual Kalman filter algorithm," Automobile Times, no. 300, pp. 59-60, Sep. 2018.
3. J. Li, "Research on lithium battery health state management under circuit fault diagnosis methods," M.S. thesis, supervised by Q. Guo, Guilin University of Electronic Technology, Guilin, China, 2020.
4. C. Wang and Q. Li, "SOC estimation of supercapacitors based on unscented Kalman filter," Power Supply Technology, vol. 45, no. 12, pp. 1624-1627, 2021.
5. Q. Yang, H. W. Sun, and F. B. Zhang, "Research on SOC estimation algorithm of lithium battery based on improved unscented Kalman filter," Mechanical Design and Manufacturing, no. 10, pp. 220-224, 2021. doi: 10.3969/j.issn.1001-3997.2021.10.049.
6. Y. Zhao and Z. Q. Pang, "Health state estimation of power batteries based on unscented Kalman filter," Foreign Electronic Measurement Technology, no. 10, pp. 136-141, 2022.
7. P. Ladpli, F. Kopsaftopoulos, and F. K. Chang, "Estimating state of charge and health of lithium-ion batteries with guided waves using built-in piezoelectric sensors/actuators," Journal of Power Sources, vol. 384, pp. 342-354, 2018. doi: 10.1016/j.jpowsour.2018.02.056.
8. X. Lai, M. Yuan, X. Tang, et al., "Co-estimation of state-of-charge and state-of-health for lithium-ion batteries considering temperature and ageing," Energies, vol. 15, no. 19, Art. no. 7416, 2022. doi: 10.3390/en15197416.
9. H. Wang, K. Ye, and S. Zhang, "Joint estimation of SOC and SOH of lithium-ion batteries based on multi-time-scale," Small and Medium-sized Enterprise Management and Technology (Late Issue), no. 09, pp. 141-144, 2019.
10. X. Yin, Y. Song, W. Liu, et al., "Multi-scale state joint estimation for lithium-ion battery," Chinese Journal of Scientific Instrument, vol. 39, pp. 118-126, 2018.
11. X. Zhang, M. Yao, R. Song, and J. Cui, "Title of the article," Journal of Jiangsu University: Natural Science Edition, vol. 43, no. 1, pp. 24-31, 2022.
12. Y. Mo, P. Ye, C. Luo, W. Xiong, and C. Yan, "SOC estimation of lithium batteries based on improved dual Kalman filter," Power Supply Technology, vol. 44, no. 5, pp. 732-735, 2020.
13. H. Li, "Research on SOC estimation of lithium batteries based on CKF," M.S. thesis, Hefei University of Technology, Hefei, China, 2018.
14. G. Li, R. Xie, S. Wei, and C. Zong, "Vehicle state and road adhesion coefficient estimation based on dual-capacity Kalman filter," Science China: Technological Sciences, vol. 0, no. 4, pp. 403-414, 2015. doi: 10.1360/n092014-00207.
15. S. J. Moura, M. Krstic, and N. A. Chaturvedi, "Adaptive PDE observer for battery SOC/SOH estimation," in Proc. Dynamic Systems and Control Conference, American Society of Mechanical Engineers, 2012, pp. 101-110. doi: 10.1115/DSCC2012-MOVIC2012-8800.
16. Y. Zhang, H. Wu, and C. Ye, "SOC estimation of lithium batteries based on IFA-EKF," Energy Storage Science and Technology, vol. 9, no. 01, pp. 117-123, 2020. doi: 10.12028/j.issn.2095-4239.2019.0127.
17. J. M. Tarascon and M. Armand, "Issues and challenges facing rechargeable lithium batteries," Nature, vol. 414, no. 6861, pp. 359-367, 2001. doi: 10.1038/35104644.
18. B. Ming and H. Han, "Progress in cathode materials for lithium-ion batteries," Chemical Production and Technology, vol. 19, no. 4, pp. 24-36, 2012.
19. A. Liu and J. Dai, "Feasibility analysis of lithium iron phosphate batteries in DC systems of nuclear power plants," Instrumentation User, vol. 30, no. 1, pp. 55-59, 2023. doi: 10.3969/j.issn.1671-1041.2023.01.013.
20. G. Xie, "Research on SOC estimation of lithium iron phosphate batteries based on unscented Kalman filter," M.S. thesis, Hefei University of Technology, Hefei, China, 2015. doi: 10.7666/d.Y2761485.
21. S. Zhang, "Modeling and state estimation of lithium iron phosphate batteries for vehicles," M.S. thesis, Wuhan University of Technology, Wuhan, China, 2018.
22. C. Wang, "Remaining charge estimation of lithium batteries based on integral Kalman filter," M.S. thesis, Xi'an University of Science and Technology, Xi'an, China, 2020.
23. Q. Deng, "Research on SOC estimation of lithium batteries based on improved EKF algorithm," M.S. thesis, Fujian University of Technology, Fujian, China, 2018.
24. L. G. Lu, X. B. Han, J. Q. Li, et al., "A review on the key issues for lithium-ion battery management in electric vehicles," Journal of Power Sources, vol. 226, pp. 272-288, 2013. doi: 10.1016/j.jpowsour.2012.10.060.
25. X. Li, C. Yuan, and Z. Wang, "Multi-time-scale framework for prognostic health condition of lithium battery using modified Gaussian process regression and nonlinear regression," Journal of Power Sources, vol. 467, Art. no. 228358, 2023. doi: 10.1016/j.jpowsour.2020.228358.
26. M. A. Hoque, P. Nurmi, A. Kumar, et al., "Data-driven analysis of lithium-ion battery internal resistance towards reliable state of health prediction," Journal of Power Sources, vol. 513, Art. no. 230519, 2021. doi: 10.1016/j.jpowsour.2021.230519.
27. X. Li, Y. Yu, Z. Zhang, and X. Dong, "External characteristics of lithium-ion power batteries based on electrochemical aging degradation model," Acta Physica

Sinica, vol. 71, no. 3, pp. 339-347, 2022. doi: 10.7498/aps.71.20211401.
28. H. Pang, "Multi-scale modeling and simplification methods of lithium-ion batteries based on electrochemical models," Acta Physica Sinica, vol. 66, no. 23, pp. 306-316, 2017. doi: 10.7498/aps.66.238801.
29. J. W. Wei, G. Z. Dong, C. B. Zhang, et al., "Review of mathematical models for power batteries used in electric vehicles," in Proc. 15th China Conference on System Simulation Technology and Its Applications (CCSSTA2014), 2014, p. 8.
30. H. Li, "Research on modeling and SOC estimation methods for lithium batteries in electric vehicles," M.S. thesis, Jilin University, Jilin, China, 2020.
31. Q. Ning, "Research on SOC prediction methods for lithium iron phosphate batteries based on improved Thevenin model," M.S. thesis, North University of China, Taiyuan, China, 2016.
32. F. Zheng, Y. Xing, J. Jiang, et al., "Influence of different open circuit voltage tests on state of charge online estimation for lithium-ion batteries," Applied Energy, vol. 183, pp. 513-525, 2016. doi: 10.1016/j.apenergy.2016.09.010.
33. H. Dai, Z. Sun, and X. Wei, "Estimation of internal state of lithium-ion power batteries for electric vehicles using dual Kalman filter algorithm," Journal of Mechanical Engineering, vol. 45, no. 6, pp. 95-101, 2009. doi: 10.3901/JME.2009.06.095.
34. J. Yao, "Research on particle filter tracking methods," Ph.D. dissertation, Chinese Academy of Sciences, Beijing, China, 2005.
35. I. Arasaratnam and S. Haykin, "Cubature Kalman filters," IEEE Transactions on Automatic Control, vol. 54, no. 6, pp. 1254-1269, 2009. doi: 10.1109/TAC.2009.2019800.
36. S. Wang, "Adaptive volume Kalman filter and its application in radar target tracking," M.S. thesis, Dalian Maritime University, Dalian, China, 2015.
37. X. Pang, R. Huang, J. Wen, et al., "A lithium-ion battery RUL prediction method considering the capacity regeneration phenomenon," Energies, vol. 12, no. 12, Art. no. 2247, 2019. doi: 10.3390/en12122247.
38. B. Zhu, X. Hu, M. He, L. Chi, and T. Xu, "Research on data mining model of fault operation and maintenance based on electric vehicle charging behavior," Frontiers in Energy Research, vol. 10, Art. no. 1044379, Jan. 2023. doi: 10.3389/fenrg.2022.1044379.
39. W. Song, X. Liu, T.-T. Li, Y. Wang, X. Zhang, C.-W. Lou, and J.-H. Lin, "The strategy of achieving flexibility in materials and configuration of flexible lithium-ion batteries," Energy Technology, vol. 9, Art. no. 2100539, Nov. 2021. doi: 10.1002/ente.202100539.